Structure and mechanical flexibility of carbon nanotube ribbons: An atomic-force microscopy study

Min-Feng Yu[a] and Mark J. Dyer
Advanced Technologies Group, Zyvex Corporation, Richardson, Texas 75081

Rodney S. Ruoff[b]
Department of Mechanical Engineering, Northwestern University, 2145 Sheridan Road, Evanston, Illinois 60208-3111

(Received 8 December 2000; accepted for publication 24 January 2001)

Collapsed multiwalled carbon nanotube (MWCNT) sections and segments (carbon nanotube ribbons) on surfaces were observed by atomic-force microscopy. The collapsed form of these MWCNTs allowed the determination of the layer number and the inner and outer diameters for their uncollapsed form. The results show that such carbon nanotube ribbons are extremely flexible and readily conform to the underlying substrate morphology. The formation of the collapsed form of these nanotubes is consistent with recent theoretical analysis on the mechanics of nanotubes. © *2001 American Institute of Physics.* [DOI: 10.1063/1.1356437]

I. INTRODUCTION

Carbon nanotubes (CNTs) are fascinating materials for nanoscale mechanical and transport properties studies. The unique structure of CNTs, a cylinder (or multiple nested cylinders) formed from a graphene sheet (or sheets) rolled each with a particular wrapping angle, determines many observed electronic properties, such as metallic or semiconducting conductivities,[1] ballistic transport properties,[2] the coulomb blockade effect,[3] the Luttinger liquid electron behavior,[4] among others. The stiff and high-enthalpy C–C bonds in the structure also determine excellent mechanical properties such as high tensile strength,[5,6] and the large Young's modulus as predicted[7] and measured.[8] Applications are projected in many areas, including nanoelectronics where CNTs can be used as nanowires, interconnects, or nanotransistors, and in materials such as high-strength reinforcing agents in composites or high-strength cabling.

While CNTs have been predicted and measured to possess high stiffness and strength along their axial direction, the hollow cylindrical structure renders CNTs susceptible to significant lateral deformation. For example, some CNTs can collapse into flattened ribbons, as first observed by transmission electron microscopy (TEM)[9] and later by atomic-force microscopy (AFM).[10,11] Theory and experiment also reveal that CNTs can be slightly or significantly deformed due to interaction with an underlying substrate or another closely contacting object.[11,12] In addition, measurements have been carried out to map quantitatively the deformability of CNTs by indentation methods using AFM.[13,14]

Due to the small size of CNTs, extensive studies of the mechanical properties of CNTs are challenging. In this work, we take advantage of the observed unique shape of collapsed multiwalled carbon nanotubes (MWCNTs) to deduce their intrinsic mechanical properties and reveal the extremely flexible nature of these CNT ribbons.

II. EXPERIMENTAL TECHNIQUES AND RESULTS

The MWCNTs used in this experiment were made from arc-discharge growth and purified by oxidation in air. The MWCNTs were then dispersed in 2-butanone by bath sonication, and subsequently the AFM sample was prepared by placing a drop of the dispersion onto a silicon wafer substrate and dried in air. Tapping-mode AFM (Nanoscope IIIa, Digital Instruments) was used to examine the sample. The operation of this mode allows application of minimum intermittent forces when acquiring images of MWCNTs.

Shown in Fig. 1(a) are typical AFM images of MWCNTs on the silicon wafer surface. Higher features appear brighter in the gray-scale image. MWCNTs having different diameters and lengths are present in the image, as well as some contamination adhering to the MWCNTs and the substrate. Two short MWCNT segments in Fig. 1(a) appear lower in height and broader in width. Figure 1(b) is a scanned close-up image of the lower-right MWCNT segment marked by an arrow in Fig. 1(a), revealing more detail. The height profile in Fig. 1(c) was taken across the MWCNT segment along the line marked in Fig. 1(b) and shows the ''pillow'' shape typical for a collapsed MWCNT.[11] The measured height of this collapsed MWCNT is 3.1 nm and the width measured between the two highest points in the height plot is 30 nm. The high flexibility of a fully collapsed MWCNT is clearly seen from the three-dimensional image, Fig. 1(d), where the end of this MWCNT (marked with an arrow) crosses over two parallel MWCNTs and closely conforms to the contours beneath it. Uncollapsed MWCNTs that cross other tubes or surface contamination do not exhibit such flexibility.

The high flexibility of MWCNT ribbons is also revealed in other cases. Figure 2(a) is an AFM image of a flattened and folded MWCNT. The height of this MWCNT is 1.9 nm,

[a]Electronic mail: mfyu@zyvex.com
[b]Electronic mail: r-ruoff@northwestern.edu

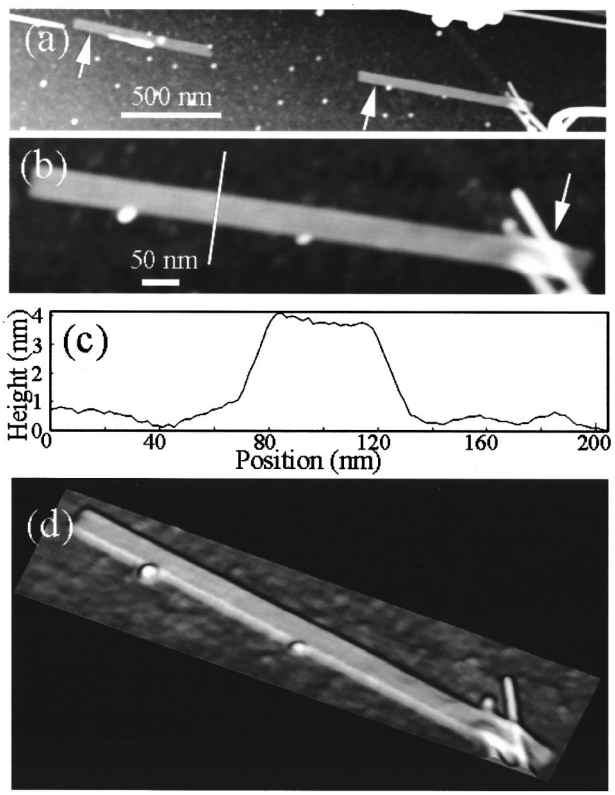

FIG. 1. (a) AFM image of two flattened MWCNT ribbons as indicated by arrows. (b) Scanned close-up image of the MWCNT ribbon marked with the arrow in the right-side of (a). (c) Height plot across the line marked in (b). (d) Three-dimensional rendering of the same flattened ribbon.

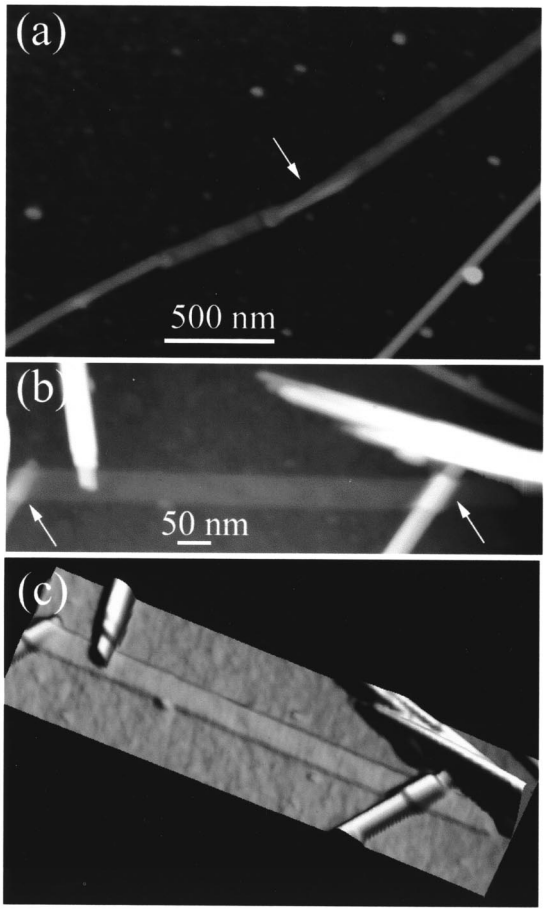

FIG. 2. (a) Twisted and then folded MWCNT ribbon. Note the apparent fold indicated by an arrow along the length of the MWCNT. (b) MWCNT ribbon crossing over underlying MWCNTs. (c) Three-dimensional image of (b) showing how the ribbon conforms remarkably closely to any change in the underlying surface, such as when crossing other MWCNTs, showing its mechanical flexibility orthogonal to the flat of the ribbon.

and the width (as defined above, namely, the distance between maxima on the ''pillow'' contour) from the height plot is 30 nm. The height obtained from the highest point along the fold (see the arrow) is 4.8 nm, slightly larger than twice the height of the flattened MWCNT, and much less than the ribbon width of 30 nm, which means that the radius of curvature of the fold should be less than 2.4 nm, half of the height of the fold. This demonstrates the great flexibility of this kind of MWCNT ribbon. Another good example is shown in Figs. 2(b) and 2(c), which are AFM images of a MWCNT ribbon crossing over two individual MWCNTs, both having a diameter of 9 nm, and the corresponding three-dimensional representation of the same ribbon, respectively. The height of this ribbon is 1.6 nm, and the width is 30 nm. The images clearly show that when the ribbon crosses over other MWCNTs, it closely follows the contour formed by the underlying MWCNTs [marked by arrows in Fig. 3(c)], demonstrating again the high flexibility of such MWCNT ribbons compared with other normal, uncollapsed MWCNT.

The dimensions of the corresponding (uncollapsed) cylinder can be obtained from the height and width of the fully collapsed MWCNT as obtained from the AFM images. Figure 3 is a schematic depicting the flattening of a three-walled CNT. From height H the number of layers of the MWCNT can be determined. From the obtained number of layers and width W, the perimeter length of the cross section can be approximately defined as $\pi(H-d)+2W$. The perimeter length determines the outer diameter R_0 of the MWCNT in its uncollapsed state, where d is the thickness assigned to each layer of the MWCNT, set equal to the interlayer distance of graphite, 0.34 nm. In the estimation above, each ''bulb'' (on left and right) in the cross section is defined as a half circle having a radius of $(H-d)/2$. The small error introduced by this simple approximation in defining the exact

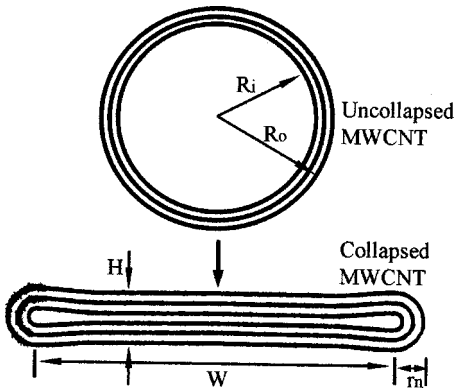

FIG. 3. Schematic showing a three-walled MWCNT in the two limiting structure cases: ideal cylinder (upper) and fully collapsed ''ribbon'' (lower).

TABLE I. Measured and calculated structural parameters for eight collapsed multiwalled carbon nanotube (MWCNT) ribbons and the calculated energy changes (ribbon vs. uncollapsed form). H is the height, W the width, and N the number of layers. N is the closest even number to $H/0.34$ for each ribbon. ID is the inner, and OD the outer, diameter. E_1 is the change in strain energy from ''bulb'' formation (per nanometer length), and E_2 is the change in strain energy per nanometer MWCNT length due to the flattened portion of the graphene layers. E_3 is the total surface energy change per nanometer MWCNT length due to the new contact area formation of the inner most layer. A negative value for E_1, E_2, or E_3 means the ribbon is stabilized relative to the cylinder.

No.	H (nm)	W (nm)	N	ID (nm)	OD (nm)	E_1 (eV)	E_2 (eV)	E_3 (eV)
1	3.1	30	10	11.3	13	45.7	−3.3	−63
2	2.0	29	6	10	11	39.4	−2.3	−61
3	1.9	30	6	11	12	39.5	−2.1	−63
4	2.1	20	6	7	8	39.2	−3.2	−42
5	1.6	30	4	11	12	34.4	−1.4	−63
6	1.6	28	4	10	11	34.4	−1.6	−59
7	1.8	12	6	5	6	38.8	−4.1	−25
8	1.8	8.5	6	4	5	38.4	−4.9	−18

geometry of MWCNT ribbons is ignored. Table I lists the structural information obtained for the eight distinct MWCNT ribbons examined here.

III. DISCUSSION

Whether a MWCNT in collapsed form is stable relative to an uncollapsed or partially collapsed form is determined by the Gibbs free energy of each form. Here, we consider the entropy contribution to the free-energy difference to be significantly less important than the enthalpy difference. We approximate the enthalpy by the internal energy and present an analysis of the energy of the fully collapsed, and separately the fully uncollapsed, forms (schematic, Fig. 3). There is an increase in energy, E_1, due to the higher curvature of the bulb regions of the graphene sheet. There is a compensating decrease in energy resulting from: (a) the flattening of the center portion of cylinders and (b) the decreased internal and external surface area of the MWCNT due to the new interlayer van der Waals contact of the inner most MWCNT cylinder, and the new contact area formed between the collapsed MWCNT and the substrate. E_1 can be defined as $\pi k/r-\pi kr/R^2$, where k is the curvature elastic modulus, 1.4 eV;[9] r is the radius of the bulb in the collapsed state, and R is the radius of the uncollapsed cylinder. The strain energy change per cylinder per unit length of the MWCNT for the flattening in the center portion, E_2, can be defined as $\pi k(R-r)/R^2$. The surface energy change per unit length of the flattened MWCNT relative to the cylindrical analogue, due to the decreased internal surface area E_3, can be defined as $2\gamma W$, and the change due to the decreased external surface area E_4 can be defined as ϕW, where γ is the surface energy of graphite, 1.05 eV/nm^2;[15] and ϕ is the work of adhesion between graphite and the SiO_2 substrate. The values of E_1, E_2, and E_3 are listed in Table I. A negative value means the ribbon form is stabilized relative to the cylinder analogue.

The value of the energy change E_4, caused by the formation of the new contact area between the MWCNT and the substrate is not assigned in Table I, due to the uncertainty of the nature of the contact between the collapsed MWCNT ribbon and the substrate. For example, a water layer may be present between the MWCNT and the substrate that may modify the CNT/substrate interaction; however, a direct contact between a collapsed MWCNT ribbon and the silicon wafer substrate yielding a significant decrease in surface energy, and thus a significant contribution by the substrate to stabilizing the ribbon, is assumed. Applying the equation for E_4 described above, the corresponding energy change estimated is -51 eV, based on the value of the work of adhesion between SiO_2 and graphite (1.7 eV/nm^2)[11] and a 30 nm width for the MWCNT ribbon. Thus, E_4 will always be negative for the ribbon versus cylinder, so the effect of the substrate/ribbon interaction is always stabilizing.

Table I thus suggests two classes of MWCNT ribbons. As noted, the SiO_2 substrate/MWCNT adhesion energy difference (stabilizing the ribbon relative to the uncollapsed cylinder) is not included in Table I. For MWCNT Nos. 1–6, the net energy change (sum of E_1, E_2, and E_3) is negative, which means that the collapse of these MWCNTs would be favored even in the absence of interaction with a substrate. For MWCNT Nos. 7 and 8, however, the net energy change for the included terms (E_1, E_2, and E_3) in the energetics analysis is positive, suggesting that these would not, in the absence of interaction with a substrate, be stable in the ribbon form. For MWCNT No. 7, an additional decrease of 10 eV per nanometer length and for No. 8, 15 eV per nanometer length would, within the energetics model employed, stabilize the ribbon form. By applying the equation for E_4, and by assuming a direct contact between the MWCNT ribbon and the substrate, the estimated contribution from the CNT/substrate interaction (E_4) for these two cases is 20 eV per nanometer for No. 7 and 14.5 eV per nanometer for No. 8. These values demonstrate the additional contribution from the substrate in stabilizing the collapse of MWCNTs to form ribbons.

Five of the eight ribbons observed in this experiment were three-walled CNTs as determined from their measured height values. The inner diameter values of these five MWCNTs for the corresponding perfect cylinders span from 4 to 11 nm. Sample Nos. 5 and 6 are two-walled CNTs having inner diameters of 11 and 10 nm, respectively. Sample No. 1 is a five-walled nanotube, having a corresponding inner diameter of 11.3 nm. According to a recent theoretical analysis supported by experimental observation of a flattened MWCNT observed by TEM,[16] the critical inner diameter for a three-walled CNT favoring collapse is between 7.0 and 12 nm, for a two-walled CNT between 5 and 10 nm, and for a five-walled CNT between 8 and 16 nm. The critical diameter favoring collapse was obtained by evaluating at what diameter the collapsed CNT has lower energy than the same CNT when uncollapsed, both in free space. An energy barrier likely exists for the intrinsic collapse (or the ''inflation'') of CNTs due to the van der Waals interactions between the opposing layers of a collapsed CNT, consequently, a collapsed state could be a higher-energy state than

the uncollapsed counterpart, and be metastable. For example, external factors could trigger collapse and the energy barrier could maintain it for some range of temperatures, if the collapsed NT is metastable. The critical diameter for metastable collapse is less than the critical diameter for stable collapse as estimated above, and the case of metastable collapse has also been analyzed in Ref. 16. Here, we have addressed the possible role of the substrate in stabilizing the collapsed form, and have demonstrated that it has a large contribution to the energetics. The model used in Ref. 16 applies to a ribbon versus cylinder in the absence of contact with a surface or other object. Our results are thus essentially in agreement with the energetics analysis presented in Ref. 16.

IV. CONCLUSION

This work demonstrates that MWCNT ribbons are extremely flexible along directions transverse to the long axis and plane of collapse. The tapping-mode AFM measurement of ribbon geometry allows assignment of the internal and outer diameters, and thus the number of nested layers, of the corresponding ideal cylinders. The MWCNTs that are observed as flattened ribbons are predicted to be stable by a model of the energetics that includes terms for strain energy in the graphene sheet (ribbon versus cylinder) and for the surface energy (ribbon versus cylinder).

It is unknown how these collapsed MWCNT ribbons are first generated. Whether they are formed prior to contact with the substrate, such as directly during the growth process, or are formed in the later handling, such as in the dispersion and transfer onto the substrate, is an open question. Telescoping of MWCNTs by application of mechanical load to inner and exposed shells has been recently reported.[5, 17,18] A fascinating possibility would be the extraction (''telescoping'') of inner shells with respect to outer shells by the action of attractive substrate forces.

ACKNOWLEDGMENTS

One of the authors (R.S.R.) appreciates research support funded by a grant through NASA Langley Research Center, Computational Materials: Nanotechnology Modeling and Simulation Program, from NSF Grant No. DMR 9871874: New Methods and Tools for Nanotechnology, and from Zyvex.

[1] T. W. Odom, J.-L. Huang, P. Kim, and C. M. Lieber, Nature (London) **391**, 62 (1998).
[2] S. J. Tans, M. H. Devoret, H. Dai, A. Thess, R. E. Smalley, L. J. Geerligs, and C. Dekker, Nature (London) **386**, 474 (1997).
[3] M. Bockrath, D. H. Cobden, P. L. McEuen, N. G. Chopra, A. Zettl, A. Thess, and R. E. Smalley, Science **275**, 1922 (1997).
[4] M. Bockrath, D. H. Cobden, J. Lu, A. G. Rinzler, R. E. Smalley, L. Balents, and P. L. McEuen, Nature (London) **397**, 598 (1999).
[5] M.-F. Yu, O. Lourie, M. J. Dyer, K. Moloni, T. F. Kelly, and R. S. Ruoff, Science **287**, 637 (2000).
[6] M.-F. Yu, B. S. Files, S. Arepalli, and R. S. Ruoff, Phys. Rev. Lett. **84**, 5552 (2000).
[7] J. P. Lu, Phys. Rev. Lett. **79**, 1297 (1997).
[8] M. M. J. Treacy, T. W. Ebbesen, and J. M. Gibson, Nature (London) **381**, 678 (1996).
[9] N. G. Chopra, L. X. Benedict, V. H. Crespi, M. L. Cohen, S. G. Louie, and A. Zettl, Nature (London) **377**, 135 (1995).
[10] R. Martel, T. Schmidt, H. R. Shea, T. Hertel, and P. Avouris, Appl. Phys. Lett. **73**, 2447 (1998).
[11] M.-F. Yu, T. Kowalewski, and R. S. Ruoff, Phys. Rev. Lett. **86**, 87 (2001).
[12] T. Hertel, R. E. Walkup, and P. Avouris, Phys. Rev. B **58**, 13870 (1998).
[13] W. Shen, B. Jiang, B. S. Han, and S.-S. Xie, Phys. Rev. Lett. **84**, 3634 (2000).
[14] M.-F. Yu, T. Kowalewski, and R. S. Ruoff, Phys. Rev. Lett. **85**, 1456 (2000).
[15] M. E. Schrader and G. I. Loeb, *Modern Approaches to Wettability (Theory and Applications)* (Plenum, New York, 1992).
[16] L. X. Benedict, N. G. Chopra, M. L. Cohen, A. Zettl, S. G. Louie, and V. H. Crespi, Chem. Phys. Lett. **286**, 490 (1998).
[17] M.-F. Yu, B. I. Yakobson, and R. S. Ruoff, J. Phys. Chem. B **104**, 8764 (2000).
[18] J. Cumings and A. Zettl, Science **289**, 602 (2000).